Shielding a Monoenergetic Photon Source for Nonproliferation Applications Analysis

C. A. Miller[a*], C.G.R. Geddes[b], S. D. Clarke[a], S. A. Pozzi[a]

[a]*Nuclear Engineering and Radiological Sciences, University of Michigan, Ann Arbor, MI 48103, USA*
[b]*BELLA Center, Lawrence Berkeley National Laboratory, Berkeley, CA 94720, USA*
[*] *Corresponding author, cmillera@umich.edu, (248)860-5734, 2355 Bonisteel Blvd., Ann Arbor, MI 48103*

Abstract

Near-monoenergetic photon sources offer appealing improvements over broad-band bremsstrahlung sources when applied to challenges in nonproliferation efforts. The use of a laser-plasma accelerator offers electrons at the energies needed for multi-MeV Thomson sources in a compact form factor. Because these electrons have energy up to approximately 0.5 GeV, many energetic photons and neutrons are created as they are dumped out of the beam line. This fact creates challenges for performing experiments to demonstrate the advantages of such a photon source for nonproliferation applications in the short term, until effective methods for decelerating the electrons are developed. To mitigate these background particles for laboratory measurements, a system of beam dumps and secondary collimators has been designed. Once background flux is reduced to the lowest practical level, it is compared to the expected flux created by the source photon beam on a lead target. This simulation mimics a nonproliferation application by predicting measured flux off-axis from an interrogated high-Z object as a surrogate for special nuclear material. Background mitigation techniques are also expanded to a mobile interrogation case. These methods allow for demonstration of nonproliferation applications of near-monoenergetic photon sources and future deployment in the field.

I. Introduction

Near-monoenergetic photon sources (MPSs) inherently improve on many of the source properties of broad-band bremsstrahlung sources which lead to problems for nonproliferation applications [1–4]. Benefits for applications include increased specificity and reduced dose for radiography of highly attenuating materials such as shielded special nuclear material (SNM) and active interrogation to induce photonuclear reactions [5]. In particular, the use of a laser plasma accelerator (LPA) creates electrons at energies needed for multi-MeV Thomson sources in a compact form factor [6]: photons of 1-9 MeV are created by scattering a laser beam from electrons accelerated to 200-500 MeV [7–11]. After interacting with the photons, the accelerated electrons must be disposed of safely.

Because the electrons are of energies up to approximately 0.5 GeV for a Thomson source, when they are bent away from the beamline and dumped into a shield a large number of secondary particles are created When these 0.5-GeV electrons are bent away from the beamline and dumped into a shield, a large number

of secondary particles are created[12]. Note that in the longer term, plasma deceleration is being developed to substantially reduce the beam dump energy [13]. This technique will be important for applications but will not be available for first experiments. The secondary particles pose problems by both obscuring measured signals from the source photons and by imparting dose to the surrounding areas. Reducing the effects of secondary particle background is important for initial laboratory experiments and future nonproliferation applications.

Dose delivery is limited in initial experiments by source capability, but future nonproliferation applications will require higher flux and hence more robust shielding for dose control. An LPA based Thomson scattering MPS is under development at the Lawrence Berkeley National Laboratory, which will test concepts for LPA-based MPSs at few-Hz repetition rates, including tests of electron beam deceleration. This source will also be used to establish requirements for scaling such a source to the kHz repetition rates needed to satisfy application flux requirements.

In this paper, we report the design of shielding scenarios optimized for the mitigation of electron-induced background for both upcoming laboratory tests and future kHz-scale application relevant sources. In the laboratory setting, a beamstop has been designed with protruding collimators to contain the resulting secondary particle flux while allowing for changes in beam direction during experimental optimization. Limiting the effect of the electron-induced background will allow for experiments demonstrating the benefits of MPSs for nonproliferation applications, including detection of signature neutrons and photons with PSD capable organic scintillators [14,15]. For future kHz-rate sources intended to address applications, a fixed tungsten beamstop with a channel to catch the electrons was designed. In the latter case, plasma deceleration has also been considered to represent a realistic potential applications scenario. A high performance, compact combination of plasma electron deceleration and shielding will be important to allow for safe use of a mobile source for nonproliferation operations in the field. In both cases, an extra layer of low atomic number neutron shielding was used to reduce the number of photoneutrons emitted.

II. Methods

MCNPX 2.7.0 [16] and MCNP6 1.0 [17] were used for a simulation study of the shielding design. An 8-MeV photon beam is simulated with a 30% FWHM, which requires electrons accelerated to 500 MeV. This energy was chosen because it is close to the maximum anticipated for nonproliferation applications [3], hence representing a realistic worst-case shielding scenario. This energy also lies at a point in SNM cross sections where photonuclear reactions are likely to be induced, and there is a strong transmission contrast between SNM and possible shielding materials such as concrete and steel [18–20]. The 8-MeV spectrum is shown in Fig. 1, illustrating the advantage in energy concentration over broadband sources. The 500-MeV electrons are bent out of the beamline by an electromagnet at an angle of 18° into a beamstop whose design

was part of this study, while the photons proceed in the forward direction with an opening half-angle of 1.75 mrad. These parameters are derived from realistic photon source simulations [6]. The electron-induced background and signal resulting from the photon beam were simulated separately to limit computational requirements. A 20 cm × 10 cm × 5 cm lead brick is placed 7 m downstream from the shielding to act as an SNM surrogate for initial possible experiments. This target is a limiting case, as the signal will increase if SNM is available for later experiments

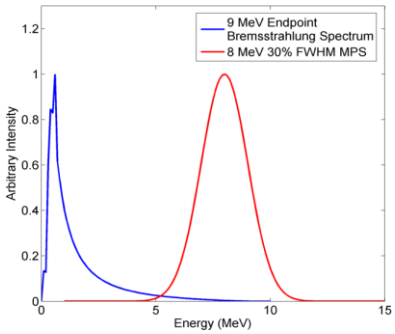

Fig. 1 Simulated 8 MeV MPS energy spectra compared to bremsstrahlung energy spectrum

III. Sources of Active Background

The high-energy electrons resulting from the accelerator source release energy in the form of photons as they are slowed down or their direction is altered [21]. The electron beam is affected by laboratory components in several different areas resulting in these energy releases.

The most significant laboratory component contributor to background is the heavy metal beamstop which limits the range of the electrons in the lab space. The electrons release their energy through bremsstrahlung which abruptly slows down the particles, and causes a release of photons up to the initial energy of the electrons [22]. Because the beamstop is constructed of a high atomic number material, the cross sections for this reaction are high. With electrons of this energy, the emission of bremsstrahlung photons is somewhat forward directed with respect to the electron beam direction, but photons are still emitted in all directions [22].

A second bremsstrahlung interaction that produces secondary photons occurs where the electrons pass through the vacuum window of the accelerator system. This interaction point is a less significant contributor than the secondary photon flux created in the beamstop because the window material is very thin and of lower atomic number than the beamstop. This fact reduces the probability for photon production, but it still considered in the shielding design.

Low-energy photons are also produced in the form of synchrotron radiation [23] where the electrons are accelerated, and again where an electromagnet bends the electrons out of the beam path. The electron bend is shown in Fig. 2. These photons are produced due to the transverse acceleration, rather than

bremsstrahlung. However, these 0.2 keV – 5keV [24,25] average energy photons are shielded by the vacuum enclosure and can therefore be neglected when designing shielding.

The photons in the active background also produce neutrons through photonuclear interactions. These photoneutrons are predominantly created in the beamstop and subsequent photon shielding because high energy photons efficiently produce photoneutrons in high atomic number materials. These photoneutrons must be considered in the shielding design, which introduces the challenge that photons and neutrons must be shielded with very different materials.

All of these effects are common to both the laboratory demonstration and mobile design for nonproliferation applications. Because the mobile design will allow for source design optimization to minimize the effects of the vacuum window radiation production only the dominant effect of the main electron beam disposal is analyzed for that case.

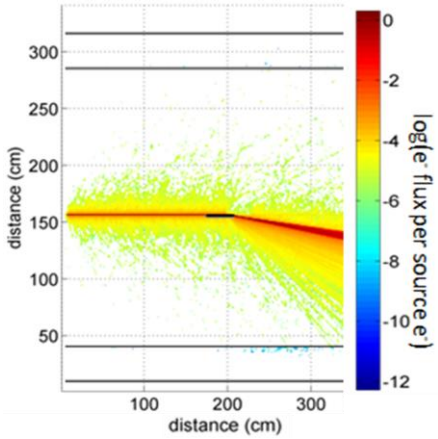

Fig. 2 Electron flux showing electrons bent out of the beamline by the 1.25 T electromagnet

IV. Shielding Design Development

Shielding has been designed to allow for safe operation and reliable results for both laboratory demonstration experiments and a future higher repetition rate mobile system. The demonstration system is being implemented at Lawrence Berkeley National Laboratory, while the mobile design is dependent on further source development and the results from the demonstration system.

A. Laboratory Design

To allow for experiments in the laboratory containing the MPS target area, we must develop shielding not only for personnel protection but also to allow for efficient detection of radiation signatures induced in a

target. This design is challenging, especially with respect to experimental background mitigation, due to space constraints and previously discussed sources of active background.

A concrete wall was initially designed as a beam dump to be sufficient for personnel protection. To further mitigate background for nonproliferation experiments, we implement a 20 cm thick wall of lead bricks proceeding and structurally supported by this concrete. Bremsstrahlung photons up to the electron energy are produced in this lead. These high energy photons are then capable of creating neutrons through photonuclear reactions. Through simulating a flux map of the laboratory, the particles in the electron interaction location were shown to be emitted in all directions, resulting in a high scattered flux throughout the room. The 20 cm lead thickness was chosen to effectively limit through-wall flux, where particles emitted from the electron interaction point on the beamstop become dominant.

To address photons emitted from the electron interaction point, a fin collimator is used (shown in Fig. 3). While a bored tube collimator would shield most effectively, it would not allow for variation of beam energy and the resulting change in bend angle. The design of the fins was iterated along with thickness of the lead wall until the limiting factor became the photons exiting back through the fin aperture, which cannot be shielded while allowing for experimental flexibility.

The fins must be about 5 cm wide to fit the full beam width, and can only be 38 cm long due to other beam components. The optimal fin configuration was determined to be 5 cm of lead, with a 5 cm thick lining of polyethylene both around the lead fins and the lead beamstop. Increasing the thickness of lead or PE has minimal effects when compared to overall scatter in the room. Using borated poly reduces the neutron flux by about 12%, but it greatly increases cost. Using a coating of a lower atomic number material than lead for the beamstop was also examined, but was shown to be ineffective for electrons of such high energy. Using this design, the fins reduce flux in the laboratory to the point where background from photons leaving the fin aperture and scattering around the laboratory dominates, and any increase in fin shielding thickness has minimal effect.

With this design, the flux maps of secondary photons and neutrons resulting from the dumped electrons are shown in Fig. 4 (a) and Fig. 4 (b). There is a large flux of photons created where the electrons interact with the lead, but these photons are shielded in the forward direction by the lead and concrete and in the reverse are effectively collimated by the fins.

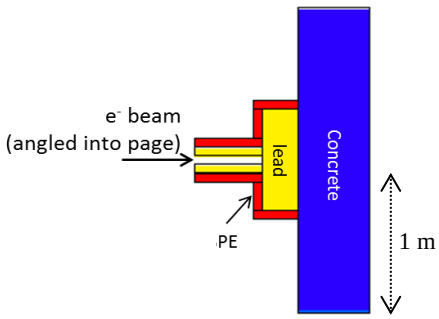

Fig. 3. LBNL MPS beamstop design. Concrete backed lead wall, with polyethylene (PE) lining.

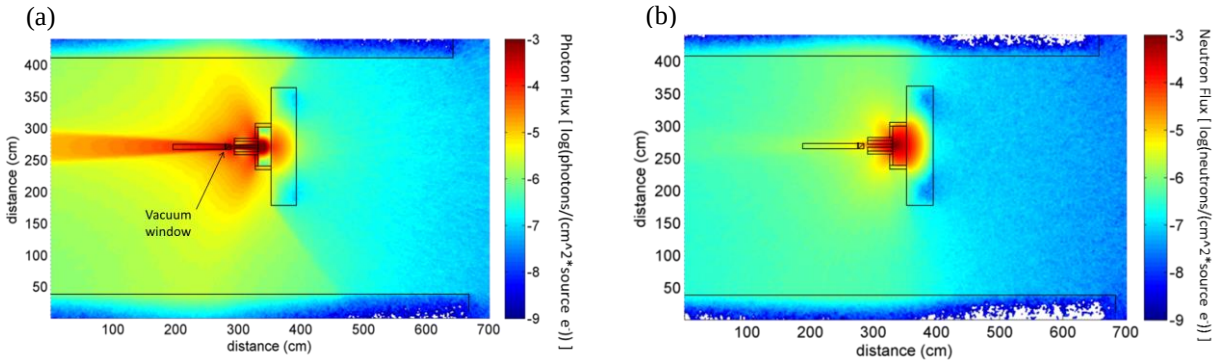

Fig. 4. Particle flux in accelerator laboratory space at the horizontal plane where the electrons impact the lead shielding for (a) photons and (b) neutrons. Effects of electron interaction with the vacuum window are included

While the neutrons are not effectively shielded by high-Z material, and easily penetrate the lead portion of the beamstop, shielding is provided by the PE layer. There are also fewer neutrons than photons initially emitted. For both particle types, the fins reduce the probability of scattering into the proposed detection area on the right side of the lab, (near 650 cm horizontally and 50 cm vertically in Fig. 4).

A comparison of the secondary particle flux on the plane of the target in the room with and without the additional fins is shown in Fig. 5. With the fins installed on the beamstop, the secondary photon flux is much more contained to the vertical plane of the electron beam. The probability of these photons scattering into the experimental area is greatly reduced compared to the case with no fins.

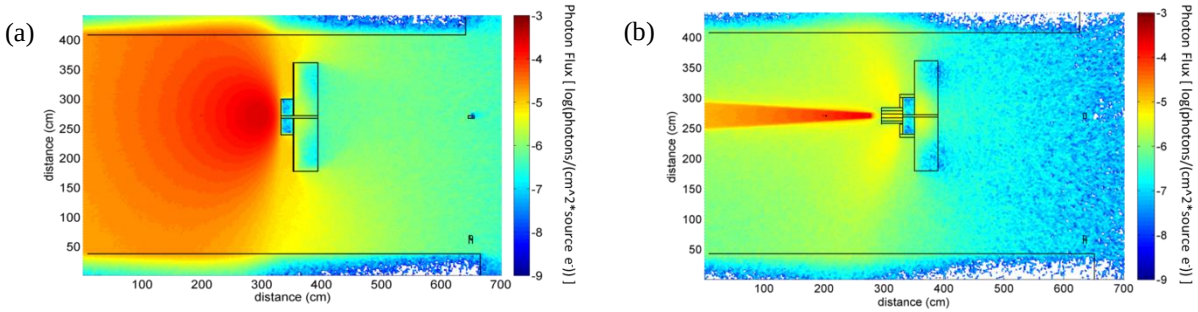

Fig. 5. Electron-induced photon flux in accelerator laboratory space at the horizontal plane of the photon target (a) without shielding fins and (b) with fins. Vacuum window effects are not included in this case

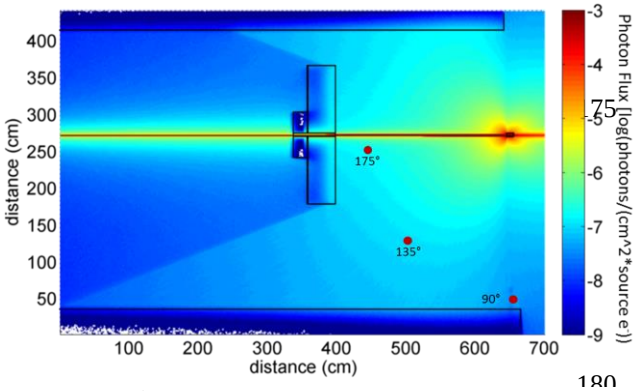

Fig. 6. Photon flux due to the MPS photon beam incident on the SNM surrogate. The beam is very tightly focused, contributing few photons to the environment until collision with the target. Point detectors shown as red dots with 45° and 0° off page

To demonstrate the relationship between this electron-induced background and the signal induced by the source, the photon beam was simulated incident on the lead brick target. As shown in Fig. 6 the photon beam anticipated from upcoming experiments [6] is highly collimated, with most of the induced photons resulting from interactions in the target. In the photon beam, the photon beam flux is much higher than that from electron induced background, which will provide good signal-to-noise for detectors assessing MPS performance.

B. Mobile Design

A mobile beamstop has been designed for potential future in-the-field nonproliferation measurements. Such measurements will require multi-kHz operation, three or more orders of magnitude greater than the laboratory setup described above. This source strength would require a very large beam dump mass (on the order of 50 metric tons of tungsten) if the full electron energy were incident on the beam dump. This very large mass requirement makes clear the need to use the plasma to decelerate the electron beam after photon production [6]. Here, the beamstop required for such a source, accounting for active plasma beam dump electron deceleration, has been evaluated. The active plasma beam dump has been simulated to allow for 90% of electrons to be decelerated to <10% initial energy [13]. This deceleration of the electrons to be

dumped allows for a large reduction in beamstop size. We have assumed that the system will have the ability to trip in the case of a plasma deceleration failure. The short pulse, high repetition rate nature of the source means that one full energy pulse contributes very little increase to the overall dose rate. Therefore this trip-on-failure assumption eliminates the need to consider additional shielding for full energy electrons at high repetition rate in the case of a failure.

The tested mobile scenario is motivated by cargo screening, cask scanning, and other applications where previous work [3] has demonstrated the need for a source producing 10^{12} photons per second for timely operation. This requirement can be achieved with a source producing 10^{8} photons per pulse with a 10 kHz repetition rate, which is in the range of future source development. This Thomson source is assumed to have a 10% electron to photon conversion rate, so 10^{13} electrons must be dumped into the beamstop.

We designed the beamstop to be as compact as possible, while limiting dose rates to less than occupational limits of 2 mrem per hour [26]. The simulated beamstop is a 1.2 m Ø × 1.2 m tungsten cylinder with a 5.08 cm Ø × 70 cm bore for the electrons to enter. Tungsten was chosen as the beamstop material because it offers an optimum combination of density and atomic number for photon attenuation among widely available materials. The tungsten cylinder is coated with ten cm of borated polyethylene for neutron shielding.

This compact beamdump design has been simulated to show that the electrons resulting from a high-flux MPS can disposed of in a manner that allows for safe field operation. Future source development to increase photon production efficiency and improve deceleration [6] may further reduce the size simulated here.

V. Shielding Performance

For a full picture of signal to background effects throughout the room, detectors were simulated 2.6 m from the target, at various angles with respect to the beam direction on the horizontal plane of the photon beam. These detector locations are represented in Fig. 6. The resulting flux values, assuming 10^{8} photons per MPS pulse, are shown in Table 1. The signal photon flux is greater than the flux of secondary photons created by dumped electrons. Due to the spatial and energy concentration of the MPS beam, even the on axis signal transmitted through the 20 cm thick lead target shown in Fig. 6 is more than fifty times the background level, indicating the ability to assess performance for thick targets. Note that these calculations do not include the effects of electron deceleration in the plasma structure, which is expected to further increase signal to background levels. The particle flux off axis is of a similar order to the electron-induced background which will be further mitigated with local detector shielding and pulse vetoing as appropriate during experiments.

Table 1. Particle flux at different locations through laboratory, resulting from electron induced background and photon beam

Angle clockwise from beam direction	Electron Induced Background (particles per [cm² * MPS pulse])		Photon Induced Signal (particles per [cm²*MPS pulse])	
	Neutron	*Photon*	*Neutron*	*Photon*
0°	1.3	3.3	0.4	226.4
45°	1.5	3.9	0.6	67.2
90°	0.8	1.1	0.7	65.3
135°	9.4	24.6	1.3	211.5
175°	8.1	30.2	0.02	291.8

The previously discussed mobile beamdump design has been simulated to show that 500-MeV electrons decelerated by ~90%, as in [13], yield photon dose rates less than a conservative limit of 1 mrem/hr on the surface of the beamdump aside from the bore location, as shown in Fig. 7. The high radiation area created by the bore will either be additionally shielded by a backstop of similar thickness or access will be restricted to that area. Using current design parameters for sources under development this design provides a concept that allows for a high-flux kHz-class MPS to be operated in the field safely with compact shielding. Greater deceleration is possible [8] and will allow for further reduction in mass.

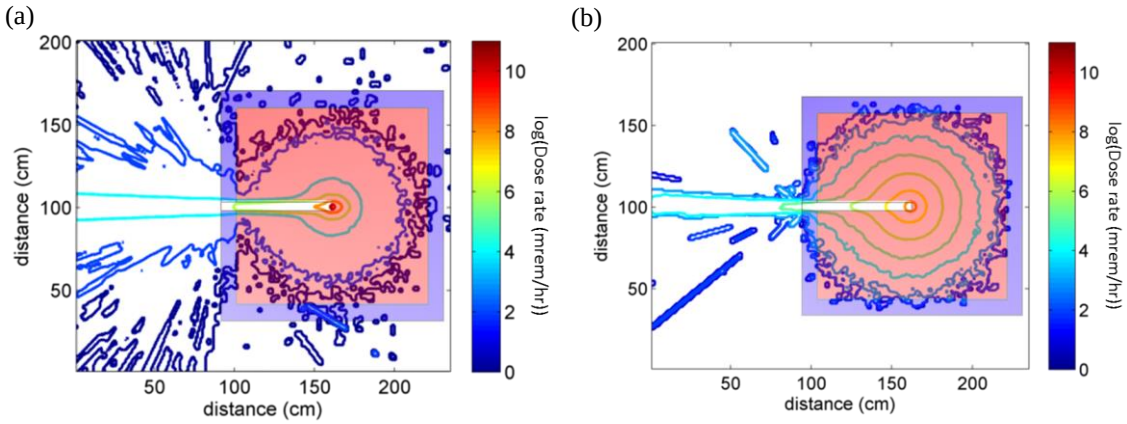

Fig. 7. Photon dose (left) and neutron dose (right) with 1.2 m diameter cylindrical mobile beamstop, 2 in. bore. Tungsten cylinder in red shaded area with BPE coating in blue

VI. Conclusions

Shielding has been designed to allow safe and effective use of MPSs both in laboratory based experiments for capability demonstrations, and a mobile scenario with nonproliferation applications. These designs consider the unique active background created by an MPS, and offer solutions mitigate it. The effects of advanced plasma deceleration are also characterized in a nonproliferation context.

In the laboratory setting a beamstop and radiation containment system was designed so that the photon flux resulting from the source signal is greater than the electron-induced background flux. The signal through a thick lead target is also many orders of magnitude greater than the active background. However, the neutron active background flux is greater than the induced signal. This laboratory shielding design has

eliminated the unwanted background as much as is practical, and with minimal neutron shielding for the detectors it will therefore be possible to detect photonuclear signals from small amounts of high-Z material.

The simulated mobile design has shown a compact shielding configuration that will allow for safe operation of an MPS in the field with a photon flux suitable for many nonproliferation applications. Plasma deceleration is important for this system to achieve the necessary flux, and further advances in that technology will lead to greater decreases in beamstop mass.

This work will allow for the experimental demonstration of advantages an MPS can offer over traditional interrogation sources in nonproliferation. With the successful demonstration of these advantages, the mobile beamdump design described here will allow for field operation of an MPS source tailored for specific nuclear nonproliferation applications.

KEYWORDS

Active interrogation; Monoenergetic photon source; Laser plasma accelerator; Photonuclear; Nonproliferation

ACKNOWLEDGEMENTS

This work was supported by the US Department of Energy, National Nuclear Security Administration Defense Nuclear Nonproliferation R&D program including work at U. Michigan through National Nuclear Security Administration award number DE-NA0002534 and at LBNL. This work was also supported by the US Department of Homeland Security, Domestic Nuclear Detection Office, Academic Research Initiative under Grant No. 2016-DN-077-ARI106, and by the Consortium for Verification Technology under Department of Energy National Nuclear Security Administration award #DE-NA0002534.

REFERENCES

[1] R.C. Runkle, D.L. Chichester, S.J. Thompson, Rattling nucleons: New developments in active interrogation of special nuclear material, Nucl. Instruments Methods Phys. Res. Sect. A Accel. Spectrometers, Detect. Assoc. Equip. 663 (2012) 75–95. doi:10.1016/j.nima.2011.09.052.

[2] J.L. Jones, J.W. Sterbentz, W.Y. Yoon, D.R. Norman, Bremsstrahlung Versus Monoenergetic Photon Dose and Photonuclear Stimulation Comparisons at Long Standoff Distances, AIP Conf. Proc. 43 (2009). doi:10.1063/1.3275665.

[3] C.G.. Geddes, B. Ludewigt, J. Valentine, B.J. Quiter, M.-A. Descalle, G. Warren, M. Kinlaw, S. Thompson, D. Chichester, C. Miller, S. Pozzi, Impact of Monoenergetic Photon Sources on Nonproliferation Applications, 2017.

[4] I. Jovanovic, A.S. Erickson, eds., Active Interrogation in Nuclear Security: Science, Technology and Systems, 1st ed., Springer, 2018.

[5] J. Chadwick, M. Goldhaber, A "Nuclear Photo-effect": Disintigration of the Diplon by Gamma-Rays, Nature. 134 (1934) 237–238. doi:10.1038/134237a0.

[6] C.G.R. Geddes, S. Rykovanov, N.H. Matlis, S. Steinke, J.L. Vay, E.H. Esarey, B. Ludewigt, K. Nakamura, B.J. Quiter, C.B. Schroeder, C. Toth, W.P. Leemans, Compact quasi-monoenergetic photon sources from laser-plasma accelerators for nuclear detection and characterization, Nucl. Instruments Methods Phys. Res. Sect. B Beam Interact. with Mater. Atoms. 350 (2015) 116–121. doi:10.1016/j.nimb.2015.01.013.

[7] H. Schwoerer, B. Liesfeld, H.P. Schlenvoigt, K.U. Amthor, R. Sauerbrey, Thomson-backscattered X rays from laser-accelerated electrons, Phys. Rev. Lett. 96 (2006) 1–4. doi:10.1103/PhysRevLett.96.014802.

[8] K. Ta Phuoc, S. Corde, C. Thaury, V. Malka, A. Tafzi, J.P. Goddet, R.C. Shah, S. Sebban, A. Rousse, All-optical Compton gamma-

ray source, Nat. Photonics. 6 (2012) 308–311. doi:10.1038/nphoton.2012.82.

[9] S. Chen, N.D. Powers, I. Ghebregziabher, C.M. Maharjan, C. Liu, G. Golovin, S. Banerjee, J. Zhang, N. Cunningham, A. Moorti, S. Clarke, S. Pozzi, D.P. Umstadter, MeV-energy X rays from inverse compton scattering with laser-wakefield accelerated electrons, Phys. Rev. Lett. 110 (2013) 1–5. doi:10.1103/PhysRevLett.110.155003.

[10] G. Sarri, D.J. Corvan, W. Schumaker, J.M. Cole, A. Di Piazza, H. Ahmed, C. Harvey, C.H. Keitel, K. Krushelnick, S.P.D. Mangles, Z. Najmudin, D. Symes, A.G.R. Thomas, M. Yeung, Z. Zhao, M. Zepf, Ultrahigh brilliance multi-MeV γ-ray beams from nonlinear relativistic thomson scattering, Phys. Rev. Lett. 113 (2014) 1–5. doi:10.1103/PhysRevLett.113.224801.

[11] H.E. Tsai, X. Wang, J. Shaw, A. V. Arefiev, Z. Li, X. Zhang, R. Zgadzaj, W. Henderson, V. Khudik, G. Shvets, M.C. Downer, Compact tunable Compton x-ray source from laser wakefield accelerator and plasma mirror, AIP Conf. Proc. 1777 (2016). doi:10.1063/1.4965663.

[12] G.R. Blumenthal, R.J. Gould, Bremsstrahlung, Synchotron Radiation, and Compton Scattering of High-Energy Electrons Traversing Dilute Gases, Rev. Mod. Phys. 42 (1973) 237–270. doi:10.1103/RevModPhys.42.237.

[13] A. Bonatto, C.B. Schroeder, J.L. Vay, C.G.R. Geddes, C. Benedetti, E. Esarey, W.P. Leemans, Passive and active plasma deceleration for the compact disposal of electron beams, Phys. Plasmas. 22 (2015). doi:10.1063/1.4928379.

[14] M.M. Bourne, S.D. Clarke, N. Adamowicz, S.A. Pozzi, N. Zaitseva, L. Carman, Neutron detection in a high-gamma field using solution-grown stilbene, Nucl. Instruments Methods Phys. Res. Sect. A Accel. Spectrometers, Detect. Assoc. Equip. 806 (2016) 348–355. doi:10.1016/j.nima.2015.10.025.

[15] N. Zaitseva, A. Glenn, L. Carman, H. Paul Martinez, R. Hatarik, H. Klapper, S. Payne, Scintillation properties of solution-grown trans-stilbene single crystals, Nucl. Instruments Methods Phys. Res. Sect. A Accel. Spectrometers, Detect. Assoc. Equip. 789 (2015) 8–15. doi:10.1016/j.nima.2015.03.090.

[16] D.B. Pelowitz, MCNPX User's Manual: Version 2.7.0, LA-CP-11-00438. (2011).

[17] J.T. Goorley, M.R. James, T.E. Booth, F.B. Brown, J.S. Bull, L.J. Cox, J.W. Durkee, J.S. Elson, M.L. Fensin, R.A. Forster, J.S. Hendricks, H.G. Hughes, R.C. Johns, B.C. Kiedrowski, S.G. Mashnik, MCNP6 User's Manual, Version 1.0, LA-CP-13-00634, Los Alamos Natl. Lab. (2013) 765.

[18] M. Frankl, R. Macián-juan, Photonuclear Benchmarks of C , Al , Cu , Ta , Pb , and U from the ENDF / B-VII Cross-Section Library ENDF7U Using MCNPX, 183 (2016).

[19] M.J. Berger, J.H. Hubbell, S.M. Seltzer, J. Chang, J.S. Coursey, R. Sukumar, D.S. Zucker, K. Olsen, XCOM: Photon Cross Sections Database, NIST Stand. Ref. Database 8 (XGAM), NIST, PML, Radiat. Phys. Div. NSBIR 87-3597. (2010). https://www.nist.gov/pml/xcom-photon-cross-sections-database.

[20] M.B. Chadwick, M. Herman, P. Obložinský, M.E. Dunn, Y. Danon, a. C. Kahler, D.L. Smith, B. Pritychenko, G. Arbanas, R. Arcilla, R. Brewer, D. a. Brown, R. Capote, a. D. Carlson, Y.S. Cho, H. Derrien, K. Guber, G.M. Hale, S. Hoblit, S. Holloway, T.D. Johnson, T. Kawano, B.C. Kiedrowski, H. Kim, S. Kunieda, N.M. Larson, L. Leal, J.P. Lestone, R.C. Little, E. a. McCutchan, R.E. MacFarlane, M. MacInnes, C.M. Mattoon, R.D. McKnight, S.F. Mughabghab, G.P. a Nobre, G. Palmiotti, A. Palumbo, M.T. Pigni, V.G. Pronyaev, R.O. Sayer, a. a. Sonzogni, N.C. Summers, P. Talou, I.J. Thompson, A. Trkov, R.L. Vogt, S.C. van der Marck, A. Wallner, M.C. White, D. Wiarda, P.G. Young, ENDF/B-VII.1 nuclear data for science and technology: Cross sections, covariances, fission product yields and decay data, Nucl. Data Sheets. 112 (2011) 2887–2996. doi:10.1016/j.nds.2011.11.002.

[21] G.F. Knoll, Radiation Detection and Measurement, 4th ed., John Wiley & Sons, Hoboken, 2010.

[22] A.L. Meadowcroft, R.D. Edwards, High-energy bremsstrahlung diagnostics to characterize hot-electron production in short-pulse laser-plasma experiments, IEEE Trans. Plasma Sci. 40 (2012) 1992–2001. doi:10.1109/TPS.2012.2201175.

[23] D.A. Edwards, M.J. Syphers, An Introduction to the Physics of High Energy Accelerators, John Wiley & Sons, 2008.

[24] S. Mobilio, F. Boscherini, C. Meneghini, Synchotron Radiation: Basics, Methods and Applications, Springer, 2015.

[25] G.R. Plateau, C.G.R. Geddes, D.B. Thorn, M. Chen, C. Benedetti, E. Esarey, A.J. Gonsalves, N.H. Matlis, K. Nakamura, S. Rykovanov, C.B. Schroeder, S. Shiraishi, T. Sokollik, J. Van Tilborg, C. Toth, S. Trotsenko, T.S. Kim, M. Battaglia, T. Stöhlker, W.P. Leemans, Low-emittance electron bunches from a laser-plasma accelerator measured using single-shot X-ray spectroscopy, AIP Conf.

Proc. 1507 (2012) 278–283. doi:10.1063/1.4773707.

[26] 10 C.F.R § 20, Standards for Protection Against Radiation, 2017.